Program Digest, 2019 IEEE International Ultrasonics Symposium (IUS)
Glasgow, Scotland, October 6-9, 2019

Practical issues on the implementation of acoustic transversal filters

Jordi Mateu
Signal Theory and Communications Dept.
Universitat Politècnica de Catalunya
Barcelona, Spain
jmateu@tsc.upc.edu

Carlos Collado
Signal Theory and Communications Dept.
Universitat Politècnica de Catalunya
Barcelona, Spain
collado@tsc.upc.edu

Robert Aigner
Qorvo
Apopka,FL USA
robert.aigner@qorvo.com

Abstract— **This paper evaluates important aspect of acoustic filters based on a transversal configuration in order to foreseen the potential and limitations of this new configuration. These aspects are: effects of the losses of the resonators and external components, such as capacitors and inductors, sensitivity on the deviation of the impedance and resonant frequency of the resonators and effects of having a non-ideal balun. This study has been performed in a sixth order filter with asymmetric position of the transmission zeros.**

Keywords— BAW, SAW, filters and electro-acoustic coupling

I. Introduction

Acoustic wave (AW) filters either in bulk or surface configuration are nowadays the dominant technology on the development of handset wireless filtering stages. The reasons for that are, without any doubt, their shrink dimensions and electrical performances in terms of insertion losses and sharp frequency roll off at the band edges. Such properties are granted by the technology itself, losses of the materials involved and frequency behaviour of the basic building blocks of a filter, the resonators [1], [2]. Smart usage of these properties leads to propose a novel filter configuration based on a transversal arrangement of the resonators forming the filter [3]-[5]. Such configuration demonstrates the possibility of achieving almost any filter response without detrimental of any dependence on the so called electro-acoustic coupling coefficient of the resonators [4]. This configuration indeed awakes the interest of exploring its limits and see how it could be applied to the demanding and new filter specifications.

This work evaluates some of the practical issues involved in the design and implementation of AW filters based on transversal configurations. In particular the present work presents two synthesized transversal networks. Equivalent circuit models will be used to evaluate the losses of the networks, where size and frequency dependence of the quality factor of the resonators will be considered. The effects of the losses will be evaluated on the in-band and on the out-of-band responses. The work will then continue with a sensitivity analysis of the networks in terms of a uniform deviation on the impedance value of resonators and a random variation on their resonant frequencies. The deviation value will be considered according real manufacturing tolerances. Evaluation of the most relevant parameters of the balun, such as the coupling value and balancing term, will be also evaluated.

II. Transversal filter configuration

The synthesized response corresponds to a sixth order filter centered at 2 GHz, with 100 MHz bandwidth and three transmission zeros (TZ), one located at the lower side band, 1.918 GHz, and two located at the upper side band, 2.086 GHz and 2.102 GHz. The characteristic polynomials describing the frequency responses have been obtained from a general Chebyshev formulation with return losses of 17.5 dB [6]. The synthesized networks are detailed in Fig. 1.

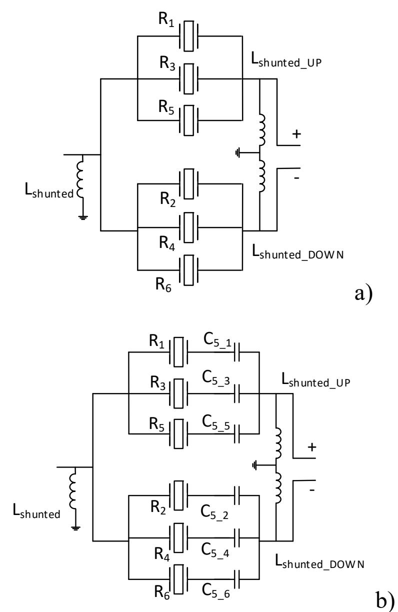

Fig. 1. Outline transversal filter topology. a) without external capacitors, b) with external capacitors.

Both networks of Fig.1 are formed by six resonators with a uniform coupling coefficient of 6.21%. The coupling coefficient is set by the designer and can be any value, even it is possible to set different resonators with different coupling [4]. In Fig. 1a, each transversal branch consists only in one resonator, whose impedance and resonant frequency are established by the synthesis of the network for a given characteristic polynomials and they cannot be controlled by the designer. We refer to this network as approach I (App.I). The resonator impedances (Z_r) are detailed in Table I. Note that their values are significantly high, which might lead to an impractical implementation [4]. The synthesized impedances of the resonators depend essentially on the proposed characteristic polynomials, the filter fractional bandwidth and the prescribed coupling coefficient of the resonators. The value of the shunt inductance ($L_{shunted}$) is 4.8 nH. Mention that $L_{shunted}$ is equal to the parallel connection of $L_{shunted\_UP}$ and $L_{shunted\_DOWN}$.

By adding a series capacitance at each branch of the network, see Fig. 1b, the designer can control the impedance of the resonators or the resonant frequency without detrimental of still prescribing the value of the coupling coefficient. For the following analysis a uniform impedance of the resonators to 50 Ω is selected. The values of the required series capacitances C_{5-i}, are listed in Table I for the corresponding resonators. This network is referred as approach II (App. II). The shunt inductance is 1.8 nH.

	App. I		App. II		
Resonator	Z_r (Ω)	Q	Z_r (Ω)	C_5 (pF)	Q
1	657	790	50	0.60	1800
2	279	1082	50	1.16	1800
3	234	1150	50	1.34	1800
4	263	1105	50	1.18	1800
5	339	1011	50	0.94	1800
6	727	760	50	0.53	1800

Table I: Synthesized values for the networks in Fig.1

III. Effects of Losses

The effects of the losses are evaluated through the limited Q of the acoustic resonators and the limited Q of the external components, which are the series capacitances C_{5_i}, (Q_C) and the shunt inductances (Q_L). The value of Q_C and Q_L are 100 and 30, respectively.

Proper modelling of the losses in the resonators needs to consider their size and therefore their impedance. For this purpose, we use an internal model described in [7], which leads to the Q values outlined in Table I, corresponding to the resonators for the filter networks in Fig.1. Note that due to the synthesized impedances, App. II leads to a uniform Q of 1800, whereas App. I leads to non-uniform and lower Q resonators.

Figure 2 shows the frequency responses of the synthesized networks when the limited Q of the resonators is considered, along with the frequency response of the characteristic polynomials when losses are accounted by a dissipative term σ [6], in blue. The value of σ in this case has been calculated from a uniform Q of 1800. Bottom plot in Fig. 2 details on the in-band insertion losses. These results reveal that the frequency response by evaluating the characteristic polynomials (blue line) and the simulated response corresponding to App.II (Fig. 1b) (solid black line), and without considering losses of external elements, overlap both in-band and near-band rejection (see details of the upper band TZ). This verifies that when uniform Q distribution exists, characteristic polynomials can be used to predict the effects of the limited Q. Inclusion of the external element losses (dash-dotted lines) produces an increment of insertion losses, and a small effect in the near band rejection.

Figure 2 also reveals that, when evaluating the network App.I (Fig. 1a) (solid red line) and therefore without uniform impedance (size) of the resonators, the frequency response shows higher insertion losses, major rounding at the band edges and lose of the TZs (see details of the upper band TZ). Note that these effects might be expected from a reduction of Q [6], however in this case the out of band performance (deepness of TZs) is significantly spoiled due to the fact that the contribution of each path is changed non-uniformly, and therefore cancellation condition to produce the transmission do not hold anymore. To verify this statement, Fig. 3 shows the filter performance with a uniform Q distribution of 500, in dash-dotted lines. Note that in this case, despite the Q reduction, the TZs are still deep enough to guarantee near band rejection, while in the case of non-uniform Q (dash-dotted red line) the effect on the TZs are further harmful. Again, overlap between the characteristic polynomial response (now for a dissipation term σ corresponding to a Q of 500) and the transversal network with external capacitor response also exists. See insertion losses details in the bottom figure (Fig.3).

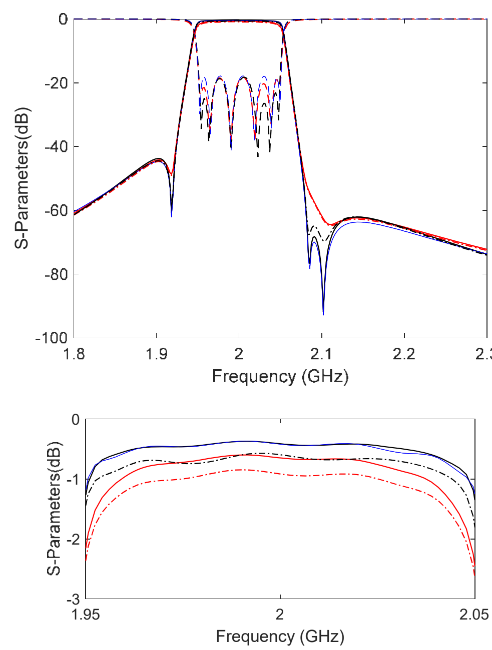

Fig. 2. Frequency response of App.I and App.II, for only resonator losses (solid lines) and with the inclusion of external losses (dash-dotted lines. Blue lines correspond to the characteristic polynomials, black lines correspond to Fig. 1b and red lines correspond to Fig.1a.

IV. Effect due to deviation on the impedance and resonant frequency of the resonators

This section performs a sensitivity analysis of the topologies in Fig 1. In particular, the sensitivity analysis evaluates the effects of varying the impedance of the resonators and their resonant frequencies. To clearer unveil these effects, losses are removed when evaluating the filter response.

Variation of the impedance of the resonators is mostly due to the manufacturing process and it happens in a uniform variation on the size of the resonators giving rise to variation up to a 1% of the resonator impedances. In contrast, variation of the resonating frequencies occurs randomly in the resonators, suffering a maximum deviation of up +/-1 MHz per resonator at the operating frequency of 2 GHz.

A. Impedance Variation

Figure 4 shows the effects of applying a uniform variation on the resonator's impedances and also on the external elements (i.e., shunt inductors and series capacitors). Although a maximum variation of 1% (solid lines) could be expected, the analysis is also applied for a 5% (dash-dotted lines) in order to extend the analysis range. Blue lines correspond to the characteristic polynomial response.

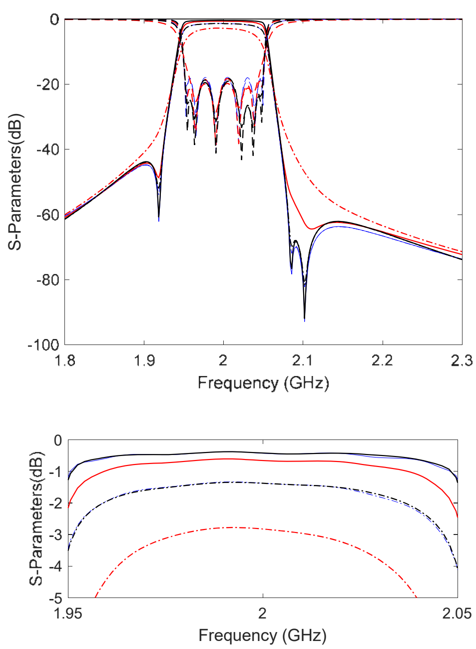

Fig. 3. Frequency response of App.I and App.II topologies when Q=1800 (solid lines) and Q=500 (dash-dotted lines). Blue lines correspond to the characteristic polynomials, black lines correspond to App.II topology (Fig. 1b) and red lines correspond to App.I topology (Fig.1a). Bottom plot details on the in-band insertion losses response.

This analysis reveals that the effects of considering a uniform variation of the impedances and all the circuit components forming the filter, barely affects the filter response. This fulfils in the near out-of-band rejection where the position and deepness of the TZs are maintained in both topologies, Fig. 1a (App. I) and Fig. 1b (App. II), and in the in-band ripple or return losses where slight deviations are observed.

Note that these results are indeed reasonable since, with a uniform variation of the resonator impedances and the external components, each signal path of the transversal configuration provides the same contribution to the overall signal.

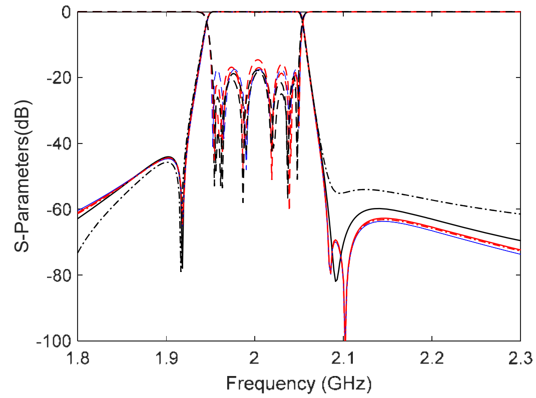

Fig. 4. Frequency response of App.I (red) and App.II (black) topologies. Blue lines correspond to the characteristic polynomials. Solid lines indicate an uniform variation of 1% on the impedances and dash-dotted line a 5%.

In dash-dotted line, Fig. 4 depicts the case without considering variation of the external components (i.e., shunt inductances and series capacitances), thus only variation of the resonator's impedances is applied. This reveals that when the impedance of the external components is not changed accordingly with the impedance of the resonator, the response in the topology of Fig. 1b deviates, especially on its near out-of-band rejection, and the position and deepness of the TZs might change and significantly reduced.

Note again that this is consistent with the fact that the contribution of each path is differently changed, therefore the out-of-band cancellation does not hold any more. Note as well, that this effect is more visible out-of-band, where small effects on each path signal contribution need to be more precise, whereas the in-band effects are barely noticeable.

B. Resonant frequency variation

As mentioned above the resonant frequency of each resonator forming the filter might deviate randomly in a +/- 1 MHz range. Instead of using a statistical analysis where hundreds of simulations would be performed by means of applying random variations, the analysis consists on performing simulation where a + 1 MHz or -1MHz deviation is applied at several resonators. This simple analysis allows to see the effects of having extreme variations at the resonant frequency of given resonators for unveil the worst cases.

Figure 5 shows the frequency responses for several scenarios. The variations applied at each simulation are indicated by means of a vector. Each position of the vector corresponds to one resonator, and the value 1 means a deviation of 1 MHz, the value -1 means a deviation of -1 MHz and the value 0 means no deviation. Mention that in this case the effect occurring in topologies App. I and App. II are equal, and only the results of App. II are depicted in Fig. 5.

The results of Fig. 5 reveal that the in-band performance is barely affected. Note that this conclusion might differ for a narrower or more stringent filter. In contrast, the simulations show that the major effect occurs out-of-band, near the band edges on the position and deepness of the TZs.

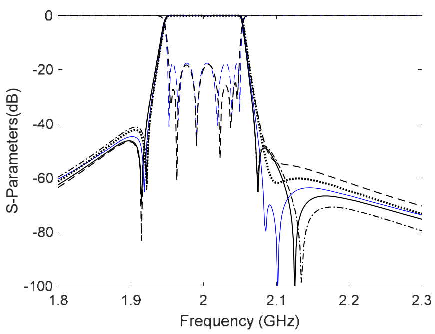

Fig. 5. Frequency response of App. II for frequency deviation of the resonators resonant frequency. The characteristic polynomial response is shown in blue. Solid line indicates to the vector variation [1 0 0 0 0 1], dashed to [1 0 0 0 0 -1], dash-dotted to [-1 0 0 0 0 1] and dotted [-1 0 1 1 0 -1].

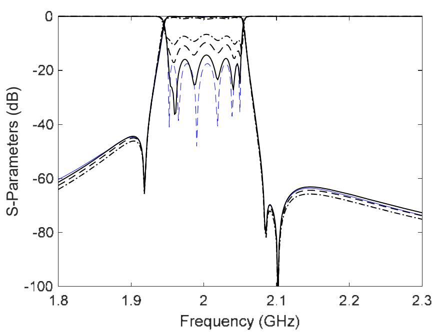

Fig. 6. Filter response for different value of coupling of the BALUN. In solid *k*=0.95, dashed *k*=0.85 and dash-dotted *k*=0.75, all in black. Blue line corresponds to the characteristic polynomials.

V. Effect of non-ideal balun

Although several effects would manifest due to the non-ideal balun behaviour, this analysis only accounts on the effect of the coupling (k) and the signal ratio (a).

A. Coupling (k) sensitivity

Figure 6 shows the effects of having a non-unitary coupling value of the balun. In particular for k=0.95, 0.85 and 0.75. Their responses are indicated in solid, dashed and dash-dotted, respectively, all in black. Blue line corresponds to the ideal response from the characteristic polynomials.

The results below reveal that the out-of-band performance is barely affected by the non-unitary coupling of the balun. This fulfils as well for the position and deepness of the transmission zeros. On the other hand, the in-band responses (or the return losses), demonstrate the existence of an expected mismatch effect. This effect can be easily recovered by changing the output matching impedance, which needs to be scaled by the value of k^2 [6].

B. Signal Ratio (a) sensitivity

The ideal value of balanced signal ratio is a =0.5. For this analysis we will perform simulation for a =0.49, 0.48, 0.47, and 0.45. Such effects are outlined in Fig. 7, in black solid, dashed, dash-dotted and dotted, respectively.

These results reveal that the unbalancing effect strongly affects the out-of-band filter performance, due to the change on how each branch contributes to the output signal. This statement can be clearly observed in Fig. 7 where the out-of-band rejection rises up to almost 20 dB.

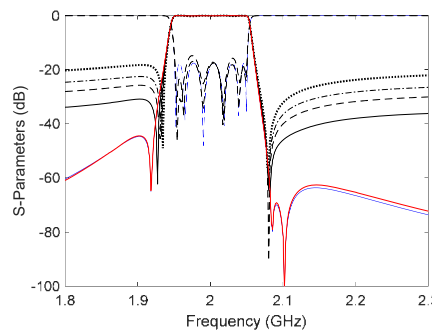

Fig. 7. Filter response for *a*=0.49, 0,48, 0.47, 0.45 in black solid, dashed, dash-dotted and dotted. Red line correspond to the response after applying the impedance scaling Blue line correspond to the characteristic polynomials.

As in the previous analysis of the k-sensitivity, one might wonder if it is possible to recover the filter performance when unbalancing effects exist. The answer is that the filter performance can be partially recovered by scaling the impedance of the resonators of the unbalanced branches by the factor a/0.5. Red line illustrates that statement. It corresponds to the response after applying the scaling factor for the case of a=0.45.

Conclusion

The analysis performed in this work concludes that transversal topologies are very sensitive to deviation on the design parameters that produce unbalancing effects between the branches. Despite of that, this topology, due to its flexibility, allows to partially recover the filter response, by modifying the external components or scaling the resonator's impedances of the transversal branches, among others.

Acknowlegments

Work supported by TEC2017-84817-C2-2-R, TEC2017-88343-C4-2-R, 2017 SGR 813, ESA- 400012413/18/NL/CRS.

References

[1] R. Ruby, "A Snapshot in Time: The Future in Filters for cells phones" *IEEE Microw. Magazine*, Vol. 16, no. 7, pp. 46-59

[2] K.Y. Hashimoto, RF Bulk Acoustic Wave Filers for Communications, 2009, Artech House.

[3] J. Mateu, C. Collado, A.Hueltes, R. Aigner, N. Khlat, Filter circuits having acoustic wave resonators in a transversal configuration, 2867-2184 Patent

[4] J.Mateu, C. Collado, A. Hueltes, R.Perea-Robles, R. Aigner, N. Khlat, "Acoustic Wave Filter for Enhanced Performance " 2018 International Ultrasonic symposium.

[5] J.Mateu, C. Collado, A. Huelter, "Novel topology for enhanced response of acoustic wave filters" Int. Micr. WS on Filters, ESA, Sept. 2018

[6] R. Cameron, et al., Microwave filters for Communications systems, John Wiley, 2007

[7] Extended BVD Model - Level 2- Qorvo Property.